1956-05

The resonance probe in a moderately high density positive column xenom plasma.

Resare, Ronald Albert

Monterey, California. Naval Postgraduate School

THE RESONANCE PROBE IN A MODERATELY HIGH DENSITY POSITIVE COLUMN XENON PLASMA

RONALD ALBERT RESARE

THE RESONANCE PROBE IN A MODERATELY HIGH DENSITY POSITIVE COLUMN XENON PLASMA

by

Ronald Albert Resare
Lieutenant, United States Navy
B. S., Purdue University, 1959

Submitted in partial fulfillment

for the degree of

MASTER OF SCIENCE IN PHYSICS

from the

UNITED STATES NAVAL POSTGRADUATE SCHOOL

May 1966

ABSTRACT

The direct current resonance probe technique was applied to a moderately high density positive column xenon discharge in the presence of moving striations. The resonance frequencies obtained were of the order of 500 megacycles per second, corresponding to electron plasma frequencies of the order of one to one and a half gigacycles per second. The results of the experiment indicate that the resonance probe technique may be a useful method for the determination of electron temperature and density, but not electron-neutral collision frequency, in moderately high density plasmas. Experimental difficulties are discussed, and recommendations for the course of future work with resonance probes are presented.

TABLE OF CONTENTS

LIST OF TABLES

LIST OF ILLUSTRATIONS

1. Introduction.

The resonance probe technique was first developed in 1960 by Takayama, Ikegami, and Miyazaki [1], as a means of quickly determining electron temperature, density, and collision frequency in a plasma.

The method consists basically of applying a high-frequency signal to a Langmuir probe and noting the behavior of the collected direct current. Referring to Figure 1, the direct current shows three distinct regions as the frequency of the applied signal is varied: the first is an increase in the dc level in the region below the resonance frequency, independent of the signal frequency, from which the electron temperature can be determined; a noticeable peak at the resonance frequency; and at higher frequencies, a rapid fall-off of the direct current to the level corresponding to no applied signal. From the position of the resonance frequency, electron plasma frequency can be calculated, and from the half-width of the peak, the electron-neutral collision frequency can be determined directly. The basic circuit for the dc resonance probe method is illustrated in Figure 2.

In this experiment, the resonance probe technique was applied to a moderately high density (on the order of 10^{10} electrons cm^{-3}) xenon positive column with pressures on the order of 10^{-3} torr).

There were major differences in the type of experimental conditions here as compared to most previous work. Most previous work has been

done in "back diffusion" plasmas, with electron densities on the order of 10^{6} cm^{-3}, and the type of gas has usually been mercury or cesium vapor. In the present investigations, in addition to the high density xenon, there were moving striations present in all ranges covered. These striations had wavelengths of seven or eight cm and frequencies of 25 - 100 kilocycles per second, with no apparent linear dependence on plasma parameters. They are ionization type waves which usually move from the anode to the cathode through the positive column [13].

2. Resonance Probe Theory.

Takayama and Ikegami [2] believed that the resonance frequency occurred at the electron plasma frequency, which is a function of electron density only:

$$(1) \qquad \omega_p = \left(\frac{4\pi n |e|^2}{m} \right)^{1/2} = 2\pi \cdot 8.97 \times 10^3 \, (n(cm^{-3}))^{1/2} ,$$

where ω_p is the electron plasma frequency, n the electron density (not necessarily constant), and e and m the electron charge and mass, respectively. Subsequent investigations [5] [7] [8] [9], however, have shown that the dc resonance peak always occurs below ω_p.

For superposed signals of form $A \cdot \sin \omega t$, below the resonance frequency, the increase in direct current is explained as follows. The electron current density, j_o, to the Langmuir probe, is given by the well-known relation:

$$(2) \qquad j_o = n \left(\frac{KT}{2\pi m} \right)^{1/2} e^{-\frac{eV}{KT}} ,$$

where K is the Boltzmann constant, T the electron temperature, and V is the potential difference between the plasma and the probe. The subscript $_o$ will refer to the current density due to the probe bias, V, which is held constant in resonance probe investigations.

The electron velocity distribution function is also assumed to be isotropic, and is determined by:

(3) $$f(v) = \frac{4m}{e^2} \quad V \frac{d^2 j}{dV^2} \quad ,$$

where v is the electron velocity.

According to Ikegami and Takayama [2], the direct current increase, δj, is then given by the second derivative of the electron current density versus potential difference curve:

(4) $$\delta j = \frac{1}{4} \quad A^2 \quad \frac{d^2 j}{dV^2} \quad .$$

If the distribution is assumed Maxwellian, the dc increase can be written:

(5) $$\delta j = j_o \left(I_o \left(\frac{eA}{KT}\right) - 1\right) \quad ,$$

where $I_o(z)$ is the zero order modified Bessel function, and A is the amplitude of the superposed signal. From this the electron temperature can be determined:

(6) $$I_o \left(\frac{eA}{KT}\right) - 1 = \frac{\delta j}{j_o} \quad .$$

For frequency ranges above the resonance frequency, the decrease in δj to zero is explained by Ichikawa [3] as being due to the effect of the oscillating potential cancelling out as an average, since the electrons cannot follow the fluctuating electric field, the transit time, τ_o, of the electrons across the probe sheath, is much longer than the period of the potential oscillation, ω^{-1}.

Solving the equation of motion for the electrons:

(7) $$m\ddot{x} = e E_o + e E_1 \sin(\omega t - \alpha) ,$$

where $E_o = \frac{V}{s}$, $E_1 = \frac{A}{s}$, s is the sheath thickness and α is a phase angle due to the plasma impedance defined by $\tan \alpha = \epsilon_r / \epsilon_i$, where ϵ_r and ϵ_i are the real and imaginary components of the plasma permittivity, respectively; and x is the distance of the electrons from the probe. Considering an electron initially at the edge of the sheath, which will require a minimum velocity v_c (hereafter called the "critical velocity") to reach the probe, leads to the following initial and boundary conditions for the solution of the equation of motion:

$$x = s, \ \dot{x} = -v \text{ at } t = 0, \text{ and } \dot{x} = 0 \text{ at } x = 0 .$$

Then the critical velocity is derived:

(8) $$v_c(\alpha, \omega) = \frac{e E_o}{m} \tau_o(\alpha) + \frac{e E_1}{m\omega} \left(\cos\alpha - \cos(\omega \tau_o(\alpha) - \alpha) \right) .$$

Then:

(9) $$j_o + \delta j = \frac{1}{2\pi} \int_o^{2\pi} \int_o^{\infty} v_c(\alpha, \omega) \, v f(v) \, dv d\alpha .$$

Solving equation (8) for the critical velocity in the low frequency region yields:

(10) $$v_1(\alpha) = \left(\frac{2e}{m} (V - A \sin\alpha) \right)^{1/2} .$$

Substitution of equation (10) into equation (8) leads to equation (5).

Integrating equation (7), one obtains:

$$(11)\quad \frac{1}{2}\,\frac{e E_o}{m}\,t^2 - s - \frac{e E_1}{m\omega}\,t\cos(\omega t - \alpha) - \frac{e E_1}{m\omega^2}\left(\sin\alpha + \sin(\omega t - \alpha)\right) = 0 .$$

In the high frequency limit, the transit time of electrons across the sheath is found from equation (11):

$$(12)\qquad \tau_o = \lim_{\omega \to \infty} (t) = \left(\frac{2ms}{e E_o}\right)^{1/2} .$$

Substituting equation (12) into equation (8), yields:

$$(13)\quad j(\omega) \equiv j_o + \delta j = j_o I_o \left(\frac{eA}{KT}\left(\frac{2eV}{m}\right)^{1/2}\frac{1}{\omega s}\right)$$

$$= j_o I_o \left(\frac{eA}{KT}(v)\frac{1}{\omega s}\right) ,$$

from which δj approaches zero as ωs becomes greater than v.

In the frequency region at and near the resonance frequency, the mechanism is not as straightforward, and no universally accepted theory is available at present. A summary of some of the existing theories which are applicable follows.

The plasma is assumed to be homogeneous, and for simplicity in development, plane parallel probe geometry is used. The plasma system can be represented schematically as in Figure 3(a), with the high frequency potential applied across the probe and a reference electrode, usually the cathode. The resulting equivalent circuit is illustrated in Figure 3(b), after Levitskii and Shashurin [4], Uramoto, et al

[5], and Mayer [6].

It has been confirmed that both the rf and dc current components show a maximum below the electron plasma frequency, and the the rf current drops to minimum near the electron plasma frequency. The former case (maximum) is interpreted as a series resonance, and the latter as a parallel resonance. Uramoto, et al [5], showed that the rf component increased monotonically at frequencies above the electron plasma frequency, while the dc component, δj, as previously discussed, drops rapidly to zero.

As the present investigations were concerned primarily with the dc resonance, the development will follow Ichikawa [3] and Ikegami and Takayama [2], realizing that the theory must be applied to the probe-plasma series capacitive circuit, and that the resonance frequency, ω_r, is not the same as the electron plasma frequency,

If an external oscillating potential is applied at a frequency near the electron plasma frequency, the much slower ions present in the sheath about the biased probe will not be able to follow the oscillating electric field and their distribution will be a function only of the probe bias, V. The electrons in the sheath, however, will follow the applied oscillating electric field and the resulting charge fluctuation in the sheath acts as an oscillating dielectric layer. The external perturbing field, E_{ext}, can be expressed as:

$$E_{ext}(x, t) = \frac{A}{s} D(x) \sin(\omega t - \alpha) , \tag{14}$$

where

$$(15) \qquad D(x) = \frac{1}{\Pi} \int_{-\infty}^{\infty} \frac{\sin ks}{k} e^{ikx} \, dk \, ,$$

where k is the wave number. When these latter equations are used to solve the linearized Boltzmann equation:

$$(16) \quad \frac{\partial f}{\partial t} + v \frac{\partial f}{\partial x} + \frac{e}{m} E \frac{\partial f_o}{\partial v} = - \frac{e}{m} E_{ext} + \frac{\partial f_o}{\partial v} + \left. \frac{\partial f}{\partial t} \right|_{coll} \, ,$$

where f_o is the distribution function in an equilibrium state and f is the perturbation due to the applied signal, and also

$$(17) \qquad \frac{\partial E}{\partial x} = 4\Pi e \int f \, dv \, ,$$

the following solution is obtained:

$$(18) \quad f(x, v, t) = \frac{e}{m} \frac{\partial f_o}{\partial v} A \int d\omega_o e^{-i\omega_o t} \left\{ \alpha (\omega_o + \omega) e^{-\alpha} - \alpha (\omega_o - \omega) e^{i\alpha} \right\}$$

$$\cdot \frac{1}{2\Pi} \int dk e^{ikx} \frac{1}{\omega_o - kv + i\nu_c} \frac{1}{\epsilon (k, \omega_o)} \frac{\sin ks}{ks} \, ,$$

where ω_o is taken as a dummy variable, and ν_c is the effective electron collision frequency.

When the mean path is much greater than the sheath thickness, the integral over k in the last equation can be estimated asymptotically:

$$(19) \quad \lim_{s \to o} \frac{1}{\Pi} \int dk e^{ikx} \frac{1}{\omega - kv + i\nu_c} \frac{1}{\epsilon (k, \omega_o)} \frac{\sin ks}{ks} = \frac{1}{\omega + i\nu_c} \frac{1}{\epsilon (o, \omega_o)} \frac{1}{s} .$$

Due to the time dependence of the perturbing rf signal, equation (9) is evaluated at t = 0, and assuming Maxwellian distribution of velocities, the total distribution function becomes:

$$(20)\quad f_{total}(v) = f_o(v) + f(x, v; t = 0)$$

$$= \frac{1}{2}\,\frac{eA}{KT}\; v\; f_o(v)\,\frac{1}{\omega s}\,\frac{\omega^2}{\omega_p^2 + \nu_c^2}$$

$$\left(\left(\frac{\epsilon_i}{\epsilon_r^2 + \epsilon_i^2} - \frac{\nu_c}{\omega_p}\,\frac{\epsilon_r}{\epsilon_r^2 + \epsilon_i^2}\right)\sin\alpha\right.$$

$$\left. - \left(\frac{\epsilon_r}{\epsilon_r^2 + \epsilon_i^2} - \frac{\nu_c\,\epsilon_i}{\omega\,(\epsilon_r^2 + \epsilon_i^2)}\right)\cos\alpha\right).$$

The real and imaginary components of the dielectric permittivity are defined by:

$$(21\,a)\qquad \epsilon_r(\omega) = 1 - \frac{\omega_p^2}{\omega^2 - \nu_c^2}$$

and

$$(21\,b)\qquad \epsilon_i(\omega) = \frac{\omega_p^2}{\omega^2 - \nu_c^2}\,\frac{2\omega\nu_c}{\omega^2 - \nu_c^2}\,.$$

Substituting equation (20) into equation (9) yields the final result:

$$(22)\quad j_o + \delta j(\omega) = j_o\, e^{\frac{eV}{KT}}\, I_o(\omega) + j_o\, e^{\frac{eV}{KT}}\,\frac{\omega_p \lambda_D}{\omega s}\,\frac{\omega^2}{\omega^2 + \nu_c^2}\cdot B\,,$$

where:

$$B = \frac{eA}{KT}\left(\left(\frac{\epsilon_i}{\epsilon_r^2+\epsilon_i^2} - \frac{\nu_c \epsilon_r}{\omega_o(\epsilon_r^2+\epsilon_i^2)}\right) S(\omega)\right.$$

$$\left. + \left(\frac{\epsilon_r}{\epsilon_r^2+\epsilon_i^2} - \frac{\nu_c}{\omega}\,\frac{\epsilon_i}{\epsilon_r^2+\epsilon_i^2}\right) C(\omega)\right)$$

where λ_D is the Debye length, and:

$$I_o(\omega) = \frac{1}{2\Pi}\int_o^{2\Pi} e^{-1/2\, x_c^2}\, d\alpha \tag{23}$$

where the dimensionless critical velocity, $x_c(\alpha, \omega) = (m/KT)^{1/2} v_c(\alpha, \omega)$, and

$$\begin{pmatrix} s(\omega) \\ c(\omega) \end{pmatrix} = \frac{1}{2\Pi}\int_o^{2\Pi}\int_{x_c(\alpha,\,\omega)}^{\infty} x^2 e^{-1/2x^2}\, dx \begin{pmatrix} \sin\alpha \\ \cos\alpha \end{pmatrix} d\alpha. \tag{24}$$

Equation (22) is a general solution for total dc collected by the probe. Using the critical velocity for the low frequency limit given by equation (10), the first term of equation (22) reduces to equation (5). If the approximation

$$\int_{x_c}^{\infty} x^2 e^{-1/2\, x^2}\, dx = x_c e^{-1/2\, x_c^2} \tag{25}$$

is taken, equation (22) reduces to:

$$\delta j = j_o \; 2 \; \frac{2\nu_c/\omega}{\left(1 - \frac{\omega_p^2}{\omega^2}\right) + 4\left(\frac{\nu_c}{\omega}\right)^2} \frac{\lambda_D}{s}\frac{\omega_p}{\omega}\left(\frac{eV}{KT}\right)^{1/2} \frac{eA}{KT} I_1\left(\frac{eA}{KT}\right). \tag{26}$$

Equation (26) can also be derived by solving the fundamental equations for linear response of the plasma electrons, equations (16) and (17), directly for dc current density, assuming that

$$\left(\frac{\partial f}{\partial t}\right)_{\text{coll}} = -\nu_c f \quad ,$$

eV/KT is much greater than one, that A/V is much less than one, and that $(\nu_c/\omega)^2$ is also much less than one.

Furthermore, if equation (26) is solved for the resonant peak height, δj_r, assuming $\omega = \omega_r = \omega_p$:

$$(27) \qquad \delta j_r = j_o \frac{1}{\sqrt{2}} \frac{\omega_p}{\nu_c} \frac{\lambda_D}{s} \left(\frac{eV}{KT}\right)^{1/2} \frac{eA}{KT} I_1\left(\frac{eA}{KT}\right) \quad ,$$

where $I_1(z)$ is the first order modified Bessel function.

The half width of the resonance peak determines the effective electron-neutral collision frequency, the relation as shown by Takayama, et al [2], is:

$$(28) \qquad \Delta\omega = 2\nu_c \quad .$$

This has been experimentally verified to within an order of magnitude by Cairns [7], using a low density mercury vapor plasma.

3. Relationship of Resonance Frequency to Electron Plasma Frequency.

As previously noted, the resonance peak of rectified current always occurs below the electron plasma frequency, and that this is due to series representation of the sheath-plasma interaction.

Mayer [6] developed a theory for plane probe geometry and calculates the complex permittivity ϵ_{eff}, of the plasma capacitor as:

$$(29) \quad \epsilon_{eff} = \epsilon_r + \epsilon_i = 1 + (\omega_r^2 - \omega_p^2) \frac{\omega^2 - \omega_r^2 + i\nu_c\omega}{(\omega^2 - \omega_r^2) + \nu_c^2\omega^2}$$

where

$$(30) \quad \omega_r^2 = \frac{2s}{p + 2s} \omega_p^2 .$$

This model has been experimentally confirmed by von Gierke, et al [8] for a low density cesium vapor plasma with unequal sheath thicknesses at the probe and reference electrode (s_1 and s_2, respectively).

Harp and Crawford [9] expanded this theory to spherical geometry and calculated:

$$(31) \quad \omega_r^2 = \frac{1}{(1 + \frac{R}{a\lambda_D})} \omega_p^2$$

where R is the spherical probe radius and $a\lambda_D$ replaces s, and a is a constant of proportionality.

4. Experimental Results and Conclusions.

The resonance probe technique was applied to a xenon positive column discharge in a 60 cm Pyrex tube of 0.8 cm inside diameter. The probe was a 0.195 mm radius right-angle cylindrical tungsten probe located halfway between an oxide coated cathode and a tungsten rod anode. Neutral gas pressures of one to four microns of mercury were used in most of the experiments with electron densities in the plasma of the order of 10^{10} cm^{-3}. Tube currents were 20, 30, and 50 milliamperes.

Early attempts to find a consistent resonant increase in collected direct current were unsuccessful. It was believed that, in accordance with Harp and Crawford [9], the probe radius was too small in relation to λ_D, thereby damping out any resonant peak. In order to eliminate this problem, a second probe was installed in the system near the right-angle probe, towards the anode. This was a thin tantalum band, two mm wide, which was mounted around the inner wall of the tube. The apparatus is diagrammed in Figure 4. After installation of this band, resonance peaks were observed, both on it, and on the original cylindrical probe, when either probe was at floating potential and the other biased near floating potential and with an applied rf signal. It would appear that the presence of the second conducting surface is essential to observance of resonance frequencies in this type of discharge in that it provides a closer reference electrode than either the anode or cathode.

The radial profile of the electron density is assumed to be parabolic, and that the electron density at the wall is approximately 60% of that at the center of the tube. A typical plot of $\delta j/j_o$ versus the applied frequency is shown in Figure 5, with results obtained from it listed in Table 1.

It was expected that density variations caused by moving striations would broaden the resonance peak. This was confirmed in all experimental conditions as illustrated in Table 2. For calculation of ν_c, the electron temperature as obtained from $d(\ln j_o) / dV$ plots was inserted into

$$\nu_c = \frac{\bar{u}}{\lambda_e} = \left(\frac{8\,KT}{\Pi\, m} \right)^{1/2} \quad (P_c\ p) \tag{32}$$

where p is the neutral gas pressure, in torr, and P_c is the probability of collision at one torr, [10], $\bar{u}$ is the average electron velocity, and λ_e is the electron mean free path.

The expected peak height, $\delta j_r / j_o$, as calculated from equation (27), did not show a consistent relation to those measured, but, instead, varied randomly. It was confirmed, however, that the magnitude of the peak height, and the dc increase observed below the resonance frequency, were proportional to the amplitude of the applied signal. The results of peak height comparisons are given in Table 3, the amplitude of the applied signal was 0.7 volts.

The results of the measurement of the resonance frequency with

respect to the calculated electron plasma frequency appear to be closer to the model of Mayer [6] than to that of Crawford and Harp [9]. As shown by von Gierke, et al [8], the sheath thickness is assumed to be a function only of the Debye length, λ_D, i.e., $s = a\lambda_D$.

For the right-angle cylindrical probe (CP), the value of a is 2.66 for closest fit of the ratio of measured ω_r to calculated ω_r, using equation (30) and ω_p obtained from $d(j_o^2)/dV$ plots. For the wall, or ring, probe (RP), the value of a is 3.5. In the latter case, ω_p is approximated by determination of the random ion current density, j_{ri}, from Langmuir probe curves, and the relation from Glasstone and Lovberg [11]:

$$n_i \approx j_{ri} (0.40\, e)^{-1} \left(\frac{2KT}{m_i}\right)^{-1/2} , \tag{33}$$

where m_i is the ion mass. This assumes charge neutrality, i.e., the ion density, $n_i = n$.

A sample of results of the above measurements is given in Table 4, and the ratio of calculated ω_r to measured ω_r is plotted against experimentally measured ω_r in Figure 6.

In the frequency region below the resonance frequency very poor agreement with theory was obtained. The increase in the dc level appeared to be independent of applied signal frequency, but a large random scatter was noticed, and, at best, only an estimate of $\delta j/j_o$ could be made. This was most probably due to drift of j_o and to the difficulty in

accurately reading the changes in the total current density, j, since $\delta j = j - j_o$ was very small. Sample values are listed in Table 5.

In the region above the resonance frequency, δj did not drop rapidly to zero, and appeared to have one or more resonance peaks. These peaks, as suggested by Ikezi and Takayama [12], may be Tonks - Dattner resonances.

Since a resonant peak can be detected even at these comparatively high densities, it is concluded that the method of resonance probes may be useful as a diagnostic technique in positive column discharges for determination of electron temperatures and densities. However, due to the presence of moving striations, it is believed that the method may yield an average collision frequency of the plasma.

5. Recommendations for Future Investigations.

In future work it is recommended that the rf current be examined with the ultimate goal of developing a simple method of direct determination of electron plasma frequency.

It is further recommended that the dc resonance probe again be attempted in the absence of a second close electrode. The problem of electron temperature determination using the resonance probe technique may be overcome if a leveled-power rf generator is obtained, and a method can be devised to eliminate the drift of j_o, and to measure only δj rather than j. The apparent resonant peaks above ω_r should be more carefully investigated to determine whether or not they do actually represent Tonks - Dattner resonances or some other phenomenon.

BIBLIOGRAPHY

1. Takayama, K., H. Ikegami, and S. Miyazaki. Phys. Rev. Letters, 5, p. 238, 1960.

2. Takayama, K., and H. Ikegami. Resonance Probes, Institute of Plasma Physics, IPPJ-10, Nagoya University, Nagoya, Japan, March, 1963.

3. Ichikawa, Y. H. Theoretical Analysis of the Characteristics of Resonance Probe, Institute of Plasma Physics, IPPJ-14, Nagoya University, Nagoya, Japan, October, 1963.

4. Levitskii, S. M., and Shashurin. Sov. Phys. - Tech. Phys. 8, p. 319, 1963.

5. Uramoto, J., J. Fujita, H. Ikegami, and K. Takayama. RF Current Component in the Resonance Probe, Institute of Plasma Physics, IPPJ-19, Nagoya University, Nagoya, Japan, October, 1963.

6. Mayer, H. M. Measurements with a Wide-Band Probe, Proceedings of the VIth International Conference on Ionization Phenomena in Gases (Paris, July 1963), Vol. 4, 1964, pp. 129-134.

7. Cairns, R. B. Measurements of Resonance Rectification using a Plasma Probe, Proc. Phys. Soc., Vol. 82, 1963, pp. 243-251.

8. von Gierke, G., G. Müller, G. Peter, and H. H. Rabben. On the Influence of Ion Sheaths upon the Resonance Behaviour of a rf Plasma Probe, Zeitschrift fur Naturforschung, Vol. 19, May, 1964, 1107-1111.

9. Harp, R. S., and F. W. Crawford. Characteristics of the Plasma Resonance Probe, Jounral of Applied Physics, Vol. 35, December, 1964, pp. 3436-3446.

10. Brode, R. B. Revs. Modern Physics, 5, 1933, p. 257.

11. Glasstone, S. and R. H. Lovberg. Controlled Thermonuclear Reactions, D. van Norstrand Company, Inc., 1960.

12. Ikezi, H., and K. Takayama. Resonances of Radio Frequency Probe in a Plasma, Institute of Plasma Physics, IPPJ-48, Nagoya University, Nagoya, Japan, March, 1966.

13. Cooper, A. W. Experiments on the Origin of Moving Striations, Journal of Applied Physics, Vol. 35, 1964, p. 2877.

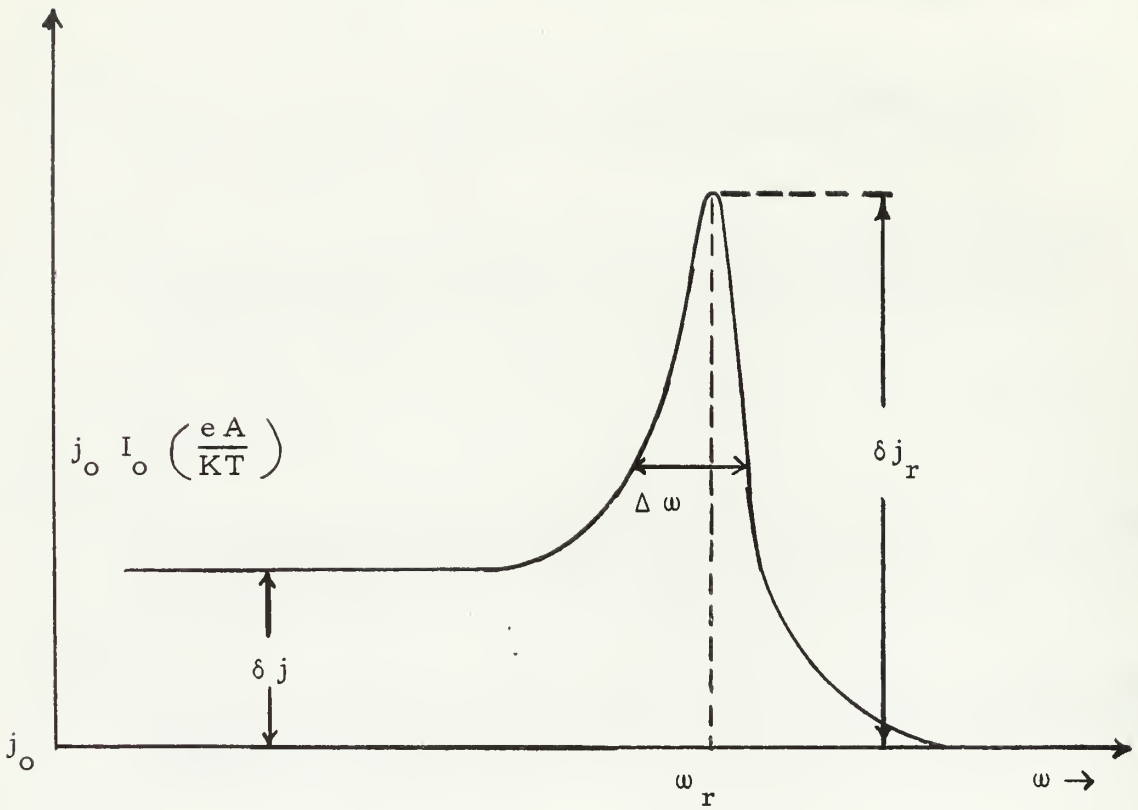

FIGURE 1

Theoretical Plot of the Increase of dc Current
Versus Frequency of the Applied rf Signal

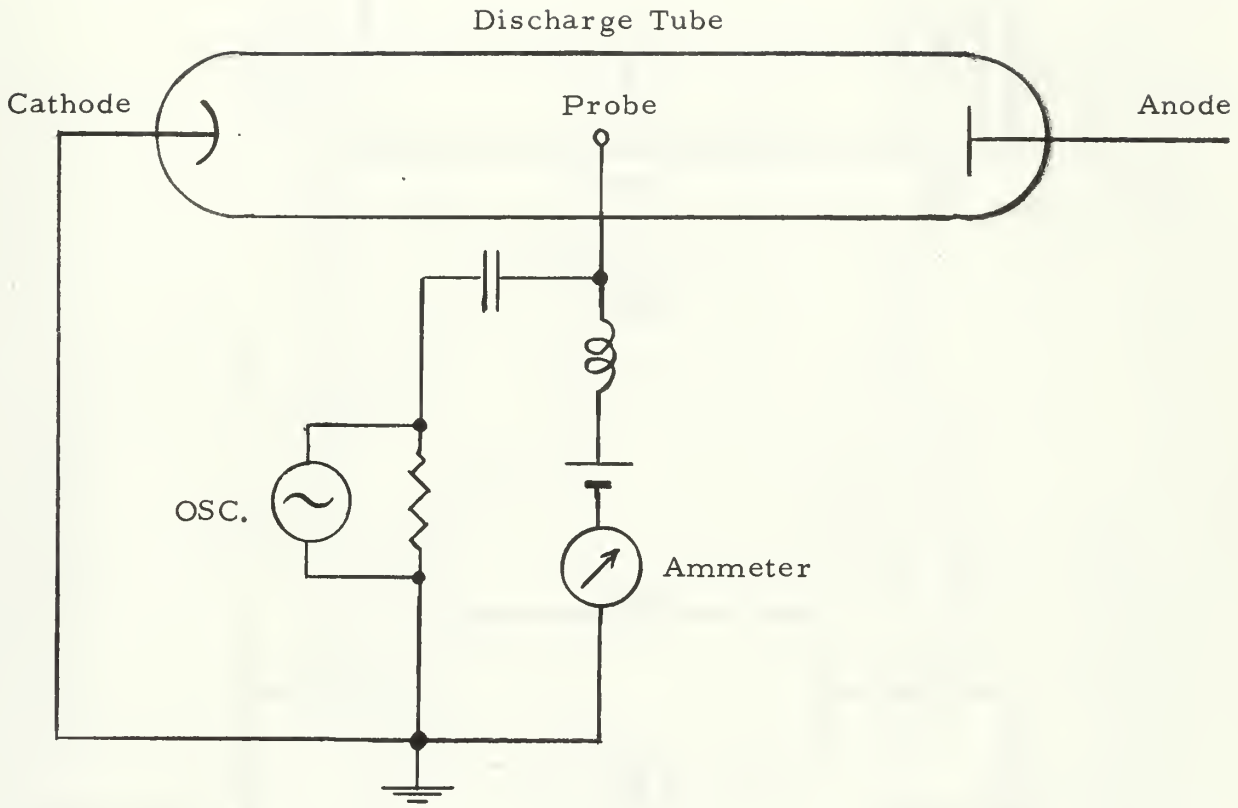

FIGURE 2

Basic Circuit for the Resonance Probe

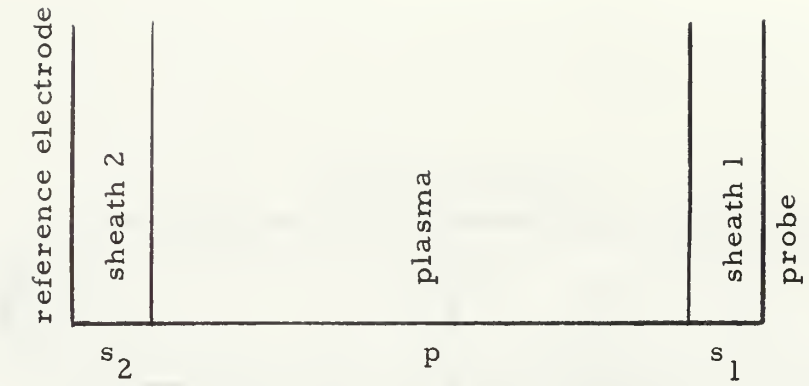

(a)

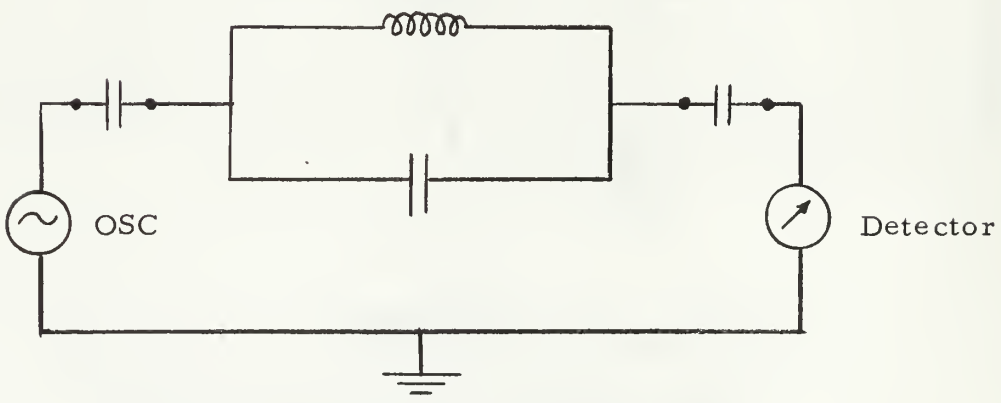

(b)

FIGURE 3

(a) The Model Proposed for the Plane Probe Plasma-Sheath System

(b) The Corresponding Equivalent Circuit

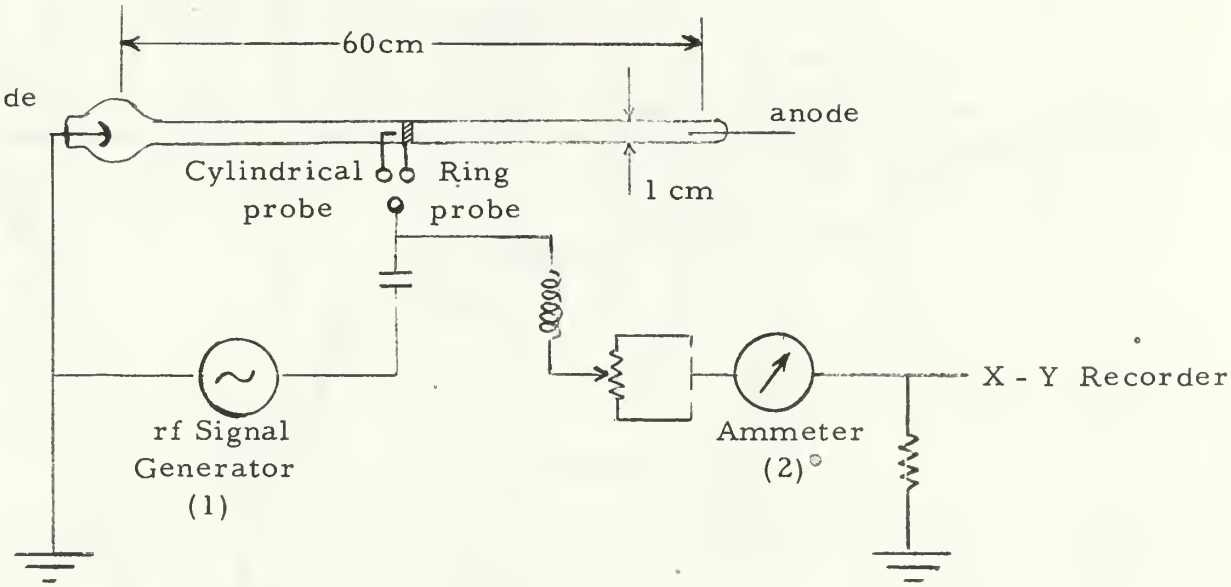

FIGURE 4

Schematic of Experimental Apparatus

Equipment Used:

(1) Signal Generators:

10-480 mc	Hewlett-Packard 608 c
450-1200 mc	Hewlett-Packard 612 a
10kc-50 mc	SG-85 / URM - 25P

(2) Ammeters:

Weston Model 430
DC Micro ammeter
Keithly Instruments
Model 600 A Electrometer

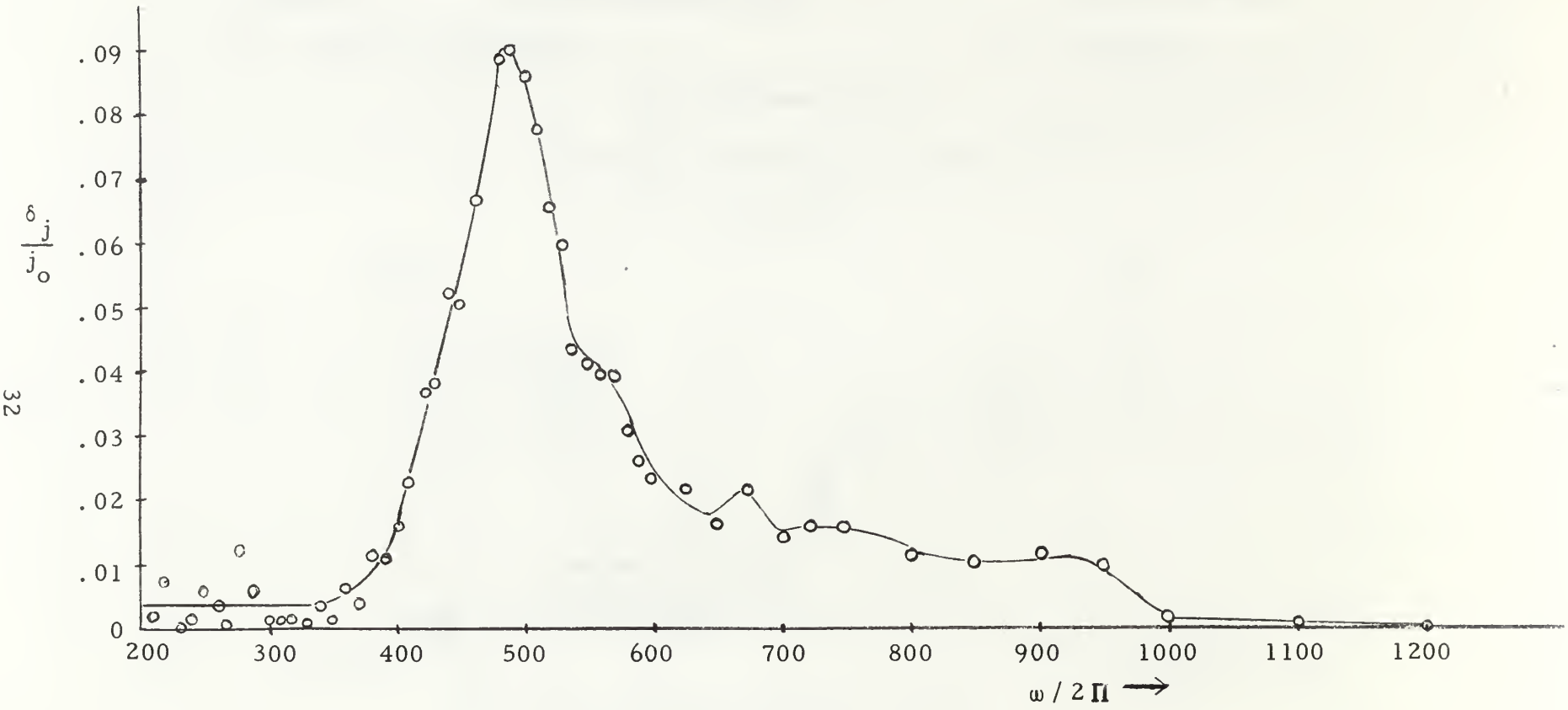

FIGURE 5

Typical Plot of $\delta j/j_o$ Versus Signal Frequency Obtained by the Resonance Probe Technique.

The gas is xenon, tube current 20 milliamperes, pressure 2.15 microns of mercury, and the probe used was the axial cylindrical probe.

TABLE 1

Analysis of Figure 5. Basic parameters are: xenon positive column discharge, pressure of 2.15 microns of mercury, and tube current 20 milliamperes.

Resonance frequency, $\omega_r / 2\Pi$:	490 megacycles per second
Half width, $\Delta \omega / 2\Pi$:	100 megacycles per second
Collision frequency, $\nu_c / 2\Pi$:	50 megacycles per second
Resonance peak height, $\delta j_r / j_o$:	0.090
Electron temperature, KT/e :	5.05 ± 1.50 ev

From the corresponding j versus V probe curve, the following comparative data is obtained:

Electron density, n :	2.22×10^{10} cm^{-3}
Electron plasma frequency, $\omega_p / 2$:	1320 megacycles per second
Collision frequency :	32.1 megacycles per second
Electron temperature :	4.05 ev
Electron Debye length, λ_D :	0.10 mm
Probe potential, V :	23 volts

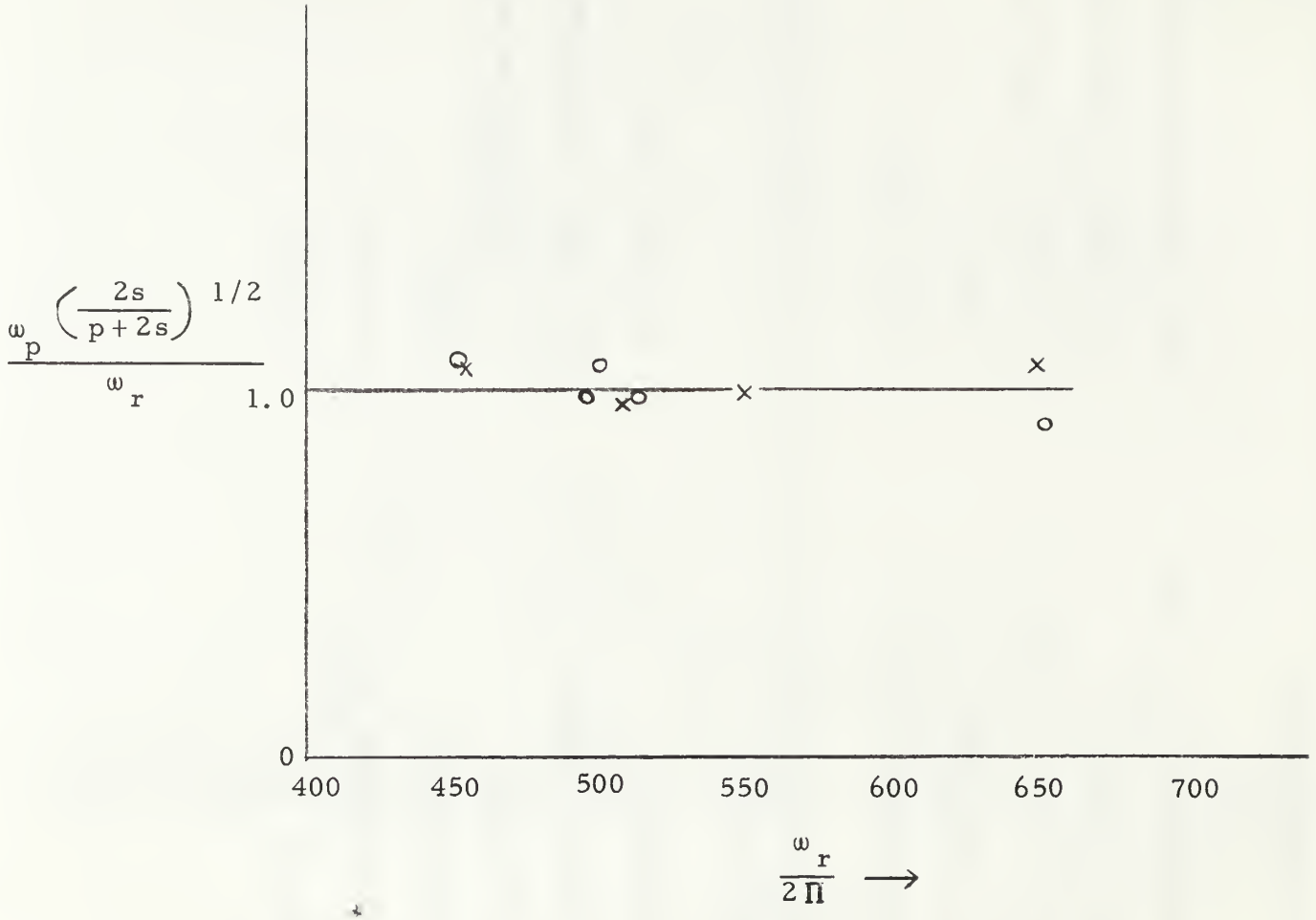

FIGURE 6

Plot of ω_r (Calculated) / ω_r (Measured) versus $\omega_r / 2\Pi$ (Measured by Resonance Probe Technique, in Megacycles per Second).

x - from ring probe data ; o - from cylindrical probe data .

TABLE 2

Representative Values of Measured Electron-Neutral Collision Frequencies and Comparison with Calculated Values (All frequencies are in megacycles per second.)

Tube Current (ma)	Pressure (microns of Hg)	Electron Density ($cm^{-3} \times 10^{-10}$)	Electron Collision Frequency		Ratio of Column 1 to 2
			Measured (1)	Calculated (2)	
		Cylindrical Probe			
20	1.6	2.22	35.0	24.8	1.41
20	2.15	2.22	50.0	32.1	1.56
20	2.4	2.18	80.0	33.5	2.39
30	3.0	3.70	86.5	31.2	2.77
50	1.8	4.36	128.5	40.5	3.17
		Ring Probe			
20	2.3	1.03	75.0	40.6	1.85
20	3.0	1.32	79.0	47.3	1.67
30	3.0	2.01	61.0	42.5	1.44
50	2.2	2.57	131.5	43.3	3.03

TABLE 3

Representative Values of Measured Resonance
Peak Height and Comparison with Calculated Values

Electron Density (cm^{-3})	Peak Height ($\delta j_r/j_o$)		Ratio of Column 2 to 1
	Measured (1)	Calculated (2)	
	Cylindrical Probe		
2.22×10^{10}	0.046	0.122	2.65
2.22×10^{10}	0.090	0.105	1.17
2.18×10^{10}	0.119	0.098	0.82
3.70×10^{10}	0.078	0.158	2.03
4.36×10^{10}	0.118	0.046	0.39
	Ring Probe		
1.03×10^{10}	0.038	0.0305	0.80
1.32×10^{10}	0.081	0.0373	0.46
2.01×10^{10}	0.053	0.0732	1.38
2.57×10^{10}	0.081	0.0425	0.525

TABLE 4

Representative Values of Measured Resonance Frequencies and Comparison with Calculated Values of Resonance Frequencies and Electron Plasma Frequency (All frequencies are given in megacycles per second.)

Electron Density (cm^{-3})	Electron Plasma Frequency (1)	Resonance Frequency		Ratio of Column 2 to 1	Ratio of Column 3 to 2
		Measured (2)	Calculated (3)		
		Cylindrical Probe			
2.22×10^{10}	1330	455	479	0.342	1.053
2.22×10^{10}	1330	490	466	0.371	0.951
2.18×10^{10}	1320	525	471	0.398	0.897
3.70×10^{10}	1720	500	519	0.290	1.038
4.36×10^{10}	1860	660	570	0.355	0.864
		Ring Probe			
1.03×10^{10}	920	460	488	0.500	1.060
1.32×10^{10}	1020	520	495	0.510	0.952
2.01×10^{10}	1270	550	545	0.433	0.991
2.57×10^{10}	1600	650	685	0.406	1.054

TABLE 5

Representative Values of Electron Temperature
as Determined by the Low Frequency Signal DC Increase
Compared with Corresponding Values from Langmuir Probe Curves

Current (ma)	Pressure (microns of mercury)	Electron Temperatures	
		Resonance Probe	Langmuir Probe
	Cylindrical Probe		
20	1.6	9.82	4.30
20	2.15	5.05	4.05
20	2.4	3.53	3.80
20	4.5	3.37	3.62
	Ring Probe		
20	1.4	7.85	4.74
20	3.0	3.54	4.34
20	4.5	6.43	4.34
50	2.3	3.93	5.63

INITIAL DISTRIBUTION LIST

		No. Copies
1.	Defense Documentation Center Cameron Station Alexandria, Virginia 22314	20
2.	Library U. S. Naval Postgraduate School Monterey, California 93940	2
3.	Defense Atomic Support Agency Department of Defense Washington, D. C. 20301	1
4.	Professor N. L. Oleson Department of Physics U. S. Naval Postgraduate School Monterey, California 93940	5
5.	Lieutenant Ronald Albert Resare, USN Box 1965, SMC U. S. Naval Postgraduate School Monterey, California 93940	1

DOCUMENT CONTROL DATA - R&D

(Security classification of title, body of abstract and indexing annotation must be entered when the overall report is classified)

1. ORIGINATING ACTIVITY *(Corporate author)*

U. S. Naval Postgraduate School
Monterey, California

2a. REPORT SECURITY CLASSIFICATION

UNCLASSIFIED

2b. GROUP

3. REPORT TITLE

THE RESONANCE PROBE IN A MODERATELY HIGH DENSITY POSITIVE COLUMN XENON PLASMA

4. DESCRIPTIVE NOTES *(Type of report and inclusive dates)*

Master's Thesis

5. AUTHOR(S) *(Last name, first name, initial)*

Resare, Ronald A., Lieutenant, United States Navy

6. REPORT DATE	7a. TOTAL NO. OF PAGES	7b. NO. OF REFS
May, 1966	38	13

8a. CONTRACT OR GRANT NO.

b. PROJECT NO.

c.

d.

9a. ORIGINATOR'S REPORT NUMBER(S)

9b. OTHER REPORT NO(S) *(Any other numbers that may be assigned this report)*

10. AVAILABILITY/LIMITATION NOTICES

11. SUPPLEMENTARY NOTES

12. SPONSORING MILITARY ACTIVITY

13. ABSTRACT

The direct current resonance probe technique was applied to a moderately high density positive column xenon discharge in the presence of moving striations. The resonance frequencies obtained were of the order of 500 megacycles per second, corresponding to electron plasma frequencies of the order of one to one and a half gigacycles per second. The results of the experiment indicate that the resonance probe technique may be a useful method for the determination of electron temperature and density, but not electron-neutral collision frequency, in moderately high density plasmas. Experimental difficulties are discussed, and recommendations for the course of future work with resonance probes are presented.

14. KEY WORDS	LINK A		LINK B		LINK C	
	ROLE	WT	ROLE	WT	ROLE	WT
Resonance Probe						

INSTRUCTIONS

1. ORIGINATING ACTIVITY: Enter the name and address of the contractor, subcontractor, grantee, Department of Defense activity or other organization *(corporate author)* issuing the report.

2a. REPORT SECURITY CLASSIFICATION: Enter the overall security classification of the report. Indicate whether "Restricted Data" is included. Marking is to be in accordance with appropriate security regulations.

2b. GROUP: Automatic downgrading is specified in DoD Directive 5200.10 and Armed Forces Industrial Manual. Enter the group number. Also, when applicable, show that optional markings have been used for Group 3 and Group 4 as authorized.

3. REPORT TITLE: Enter the complete report title in all capital letters. Titles in all cases should be unclassified. If a meaningful title cannot be selected without classification, show title classification in all capitals in parenthesis immediately following the title.

4. DESCRIPTIVE NOTES: If appropriate, enter the type of report, e.g., interim, progress, summary, annual, or final. Give the inclusive dates when a specific reporting period is covered.

5. AUTHOR(S): Enter the name(s) of author(s) as shown on or in the report. Enter last name, first name, middle initial. If military, show rank and branch of service. The name of the principal author is an absolute minimum requirement.

6. REPORT DATE: Enter the date of the report as day, month, year, or month, year. If more than one date appears on the report, use date of publication.

7a. TOTAL NUMBER OF PAGES: The total page count should follow normal pagination procedures, i.e., enter the number of pages containing information.

7b. NUMBER OF REFERENCES: Enter the total number of references cited in the report.

8a. CONTRACT OR GRANT NUMBER: If appropriate, enter the applicable number of the contract or grant under which the report was written.

8b, 8c, & 8d. PROJECT NUMBER: Enter the appropriate military department identification, such as project number, subproject number, system numbers, task number, etc.

9a. ORIGINATOR'S REPORT NUMBER(S): Enter the official report number by which the document will be identified and controlled by the originating activity. This number must be unique to this report.

9b. OTHER REPORT NUMBER(S): If the report has been assigned any other report numbers *(either by the originator or by the sponsor)*, also enter this number(s).

10. AVAILABILITY/LIMITATION NOTICES: Enter any limitations on further dissemination of the report, other than those imposed by security classification, using standard statements such as:

(1) "Qualified requesters may obtain copies of this report from DDC."

(2) "Foreign announcement and dissemination of this report by DDC is not authorized."

(3) "U. S. Government agencies may obtain copies of this report directly from DDC. Other qualified DDC users shall request through _____."

(4) "U. S. military agencies may obtain copies of this report directly from DDC. Other qualified users shall request through _____."

(5) "All distribution of this report is controlled. Qualified DDC users shall request through _____."

If the report has been furnished to the Office of Technical Services, Department of Commerce, for sale to the public, indicate this fact and enter the price, if known.

11. SUPPLEMENTARY NOTES: Use for additional explanatory notes.

12. SPONSORING MILITARY ACTIVITY: Enter the name of the departmental project office or laboratory sponsoring *(paying for)* the research and development. Include address.

13. ABSTRACT: Enter an abstract giving a brief and factual summary of the document indicative of the report, even though it may also appear elsewhere in the body of the technical report. If additional space is required, a continuation sheet shall be attached.

It is highly desirable that the abstract of classified reports be unclassified. Each paragraph of the abstract shall end with an indication of the military security classification of the information in the paragraph, represented as *(TS), (S), (C), or (U)*.

There is no limitation on the length of the abstract. However, the suggested length is from 150 to 225 words.

14. KEY WORDS: Key words are technically meaningful terms or short phrases that characterize a report and may be used as index entries for cataloging the report. Key words must be selected so that no security classification is required. Identifiers, such as equipment model designation, trade name, military project code name, geographic location, may be used as key words but will be followed by an indication of technical context. The assignment of links, roles, and weights is optional.

Thesis
R36
c.1

87091

Resare
The resonance probe in a moderately high density positive column xenon plasma.